Int. J. Chem. Sci.: 11(2), 2013, 797-814
ISSN 0972-768X
www.sadgurupublications.com

ADSORPTION OF BASIC YELLOW DYE FROM AQUEOUS SOLUTIONS BY ACTIVATED CARBON DERIVED FROM WASTE APRICOT STONES (ASAC): EQUILIBRIUM, AND THERMODYNAMIC ASPECTS

AYAD F. ALKAIM* **and MOHAMMED B. ALQARAGULY**

Department of Chemistry, Faculty of Girls Science, Babylon University, HILLA, IRAQ

ABSTRACT

The preparation of activated carbon from apricot stone (ASAC) with H_2SO_4 activation and its ability to remove a basic dye, basic yellow 28, from aqueous solutions were reported in this study. The adsorbent before and after adsorption was characterized by FTIR, and SEM, respectively. The effects of various experimental parameters, such as initial dye concentration, pH, adsorbent dosage and temperature were investigated in a batch-adsorption technique. The optimum conditions for removal of the basic dye were found to be pH 10. Fourth adsorption isotherms were used to model the equilibrium adsorption of basic yellow 28 on ASAC adsorbent (Langmuir, Freundlich, Redlich–Peterson and Langmuir-Freundlich). By considering the experimental results and adsorption models applied in this study, it can be concluded that equilibrium data were represented well by all isotherm equations under study. Thermodynamic parameters were also evaluated, which indicated that this process was spontaneous and endothermic.

Key words: Adsorption, Isotherm, Apricot stones, Basic yellow 28.

INTRODUCTION

Many fields of up-to-date technology, including the textile industry, use synthetic dyes to color their products[1]. Dyes are water-soluble and intensely colored substances used for the coloration of various substrates, including paper, leather, hair, food, cosmetics, and textiles[2]. Color removal from industry or domestic effluents has drawn considerable attention in the last few years, because of its toxicity and visibility[3]. Basic Yellow 28 (BY 28) is cationic dye, which is among the most commonly used dyestuff to dye cotton and polyacrylonitrile, and is therefore common industrial pollutants[4,5]. Various technologies including chemical oxidation, biological treatment, coagulation–flocculation, and membrane processes are currently effective methods for reducing dye concentrations in wastewater[6,7].

---

*Author for correspondence; E-mail: ayad_alkaim@yahoo.com

However, these treatment processes are costly and cannot effectively be used to treat a wide range of dye-containing wastewater. Adsorption has been found to be superior to other techniques for pollutant removal from wastewater[8,9]. Adsorption is the process by which a solid adsorbent can attract a component in water to its surface and form an attachment via a physical or chemical bond, thus removing the component from the fluid phase. The advantages of adsorption process are simplicity in operation, inexpensive compared to other separation methods and no sludge formation. Over the years, a number of workers have used different waste materials such as sawdust fly ash[10], bagasse fly ash[10,11], blast furnace slag[12], deoiled soya[13], sawdust[14], rice husk[15], rice hull[16], sugarcane dust[17], hazelnut shell[18], coir pith[19], kernel shell[20], corncob and barley husk[21] and apricot stones[4,22,23] from industrial and agricultural products as adsorbent for the removal of different pollutants from aqueous solutions.

In the present work, the adsorption characteristics of basic yellow 28 were investigated using apricot stones activated carbon ASAC as adsorbent. The adsorption isotherms and thermodynamics of the adsorbent were measured. Equilibrium data were fitted to Langmuir, Freundlich, Redlich–Peterson, and Langmuir-Freundlich equations to determine the correlation between the isotherm models and experimental data. Thermodynamic parameters were calculated to determine the adsorption mechanism. The influence of initial dye concentration, pH, dosage, and temperature on dye removal was also studied.

EXPERIMENTAL

Chemicals and reagents

Sandocryl gold yellow (Basic yellow 28) was product number 14345 supplied from Hilla Factory for textiles industries, Iraq, it was used as received. Dye solutions with concentration 50 mg L^{-1} were prepared in purified water obtained from a Milli-Q reagent grade water system.

Table 1: Textile dye Basic yellow 28 and abbreviation used in this study

Code	Structure formula[24]	Commercial name	Color index	λ_{max} (nm)	M
SLY	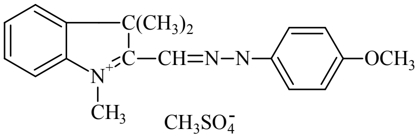	Golden yellow sandocryl	Basic yellow 28	452	433

Preparation of activated carbon from waste apricot stones

Apricot stones were obtained from Hilla city, Iraq. The material was crashed and sieved to a size range of 2.0 mm × 0.5 mm particle size prior to activation. Chemical activation using H_2SO_4 at moderate temperatures produces a high surface area and high degree of microporosity[4]. The materials were mixed in a 2 : 1 wt ratio with concentrated H_2SO_4, placed in an oven and heated to 500°C for 2 h. After this, the samples were allowed to cool to room temperature, washed with distilled water and soaked in 1% $NaHCO_3$ solution to remove any remaining acid. The samples were then washed with distilled water until pH of the activated carbon reached 6, dried at 105°C for 5 h and sieved to obtain the desired particle size (≤ 75 μm).

Adsorption experimental methods and measurements

The effects of experimental parameters, initial dye concentration (2–16 $mg.L^{-1}$), pH (varied between 3–10), adsorbent dosage (varied froms 5–50 mg/100 mL), temperature (10–40°C) and particle size ≤ 75 μm on the dye adsorption were studied in a batch mode of operation for a contact time of 60 min. The effect of pH was studied by adjusting the pH of the dye solution by adding 0.1 N HCl or 0.1 N NaOH. The solution and solid phase were separated by centrifugation at 3500 rpm for 10 min in a Hettich EB 21 centrifuge, repeated two times to ensure there is no particles scattered the absorbance measurements and analyzed using a UV–vis spectrophotometer at a wavelength of 452 nm. The final concentration of the solution was then determined from the calibration curve.

The concentration retained in the adsorbent phase ($qe/mg.g^{-1}$) was calculated by using the following equation:

$$qe = \frac{(C_o - C_e)\,V}{W_s} \quad \ldots(1)$$

where C_0 is the initial dye concentration and C_e is the equilibrium dye concentration ($mg.L^{-1}$), V is the volume of solution (l) and W_s is the mass of the adsorbent (g), also the percentage of dye removed (R%) from solution was calculated using the following equation:

$$R\,(\%) = \frac{(C_o - C_e)}{C_o} \text{ x } 100 \quad \ldots(2)$$

RESULTS AND DISCUSSION

Characterization of the adsorbent material

FT-IR characterization

The ASAC was characterized by FT-IR spectroscopy. FT-IR spectra were collected in the mid -IR range from 4000 to 400 cm^{-1} with a resolution of 1 cm^{-1}. The FT-IR spectra of ASAC before and after adsorption of BY-28 are shown in Fig. 1. The FT-IR pattern shows reduced in an intensity of bands after adsorption, also there is a real difference between ASAC before and after interaction with BY-28 which has been suggested a physical adsorption phenomenon occurs as a result of attractive forces between the ASAC surface and BY-28 under investigation[25].

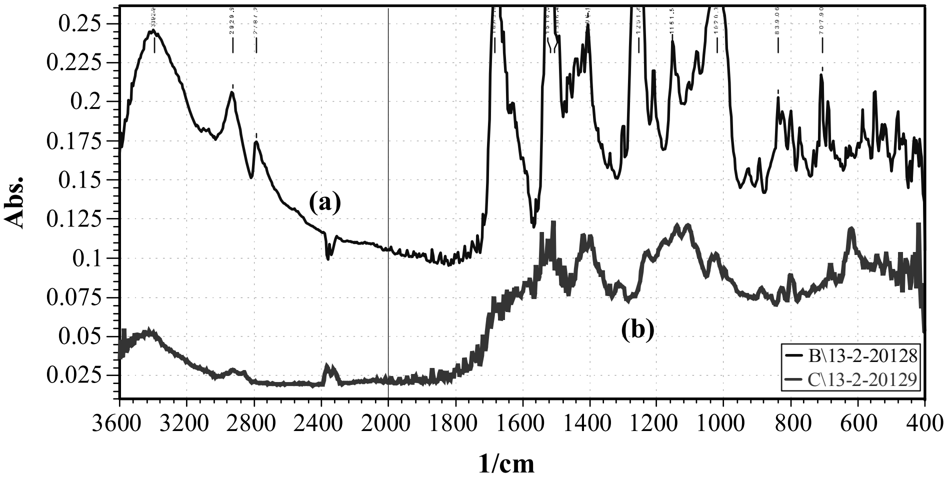

Fig. 1: FT-IR spectra of activation carbon of apricot stones (a) before, and (b) after adsorption of BY-28 dye

SEM analysis

The surface of adsorbent was also characterized by scanning electron microscopy (SEM) before and after the adsorption experiments using the dye.

SEM images of the ASAC (Figure 2(a)) showed bright dark color on the surface. After BY-28 dye adsorption the surface of the ASAC was turned to light color (Figure 2(b)). This may be due to the adsorption of BY-28 dye on the surface of the ASAC.

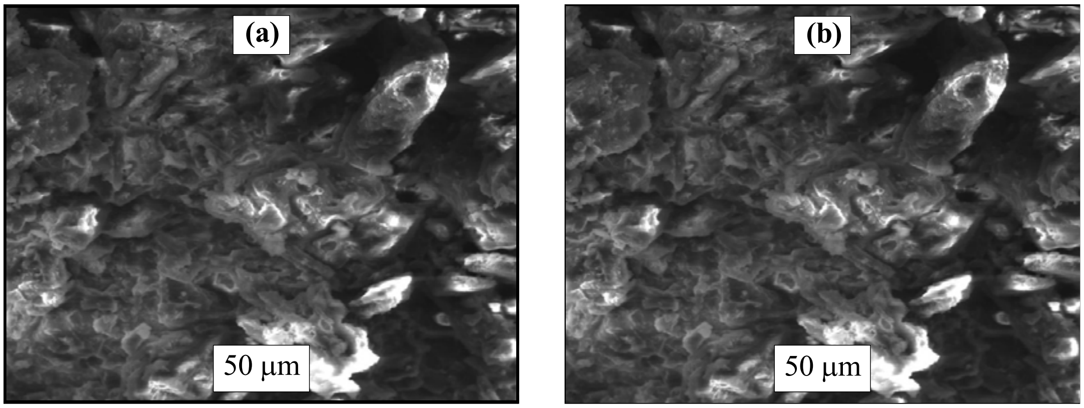

Fig. 2: SEM image of activated carbon of apricot stones (a) before and (b) after adsorption of BY-28 dye

Effect of adsorption parameters

Effect of pH

Adsorption of the dye by the ASAC is dependent upon the pH of the initial dye solution. The effect of initial pH of the dye solution on the adsorption capacity and the removal percentage (R%) of the ASAC is presented in Fig. 3.

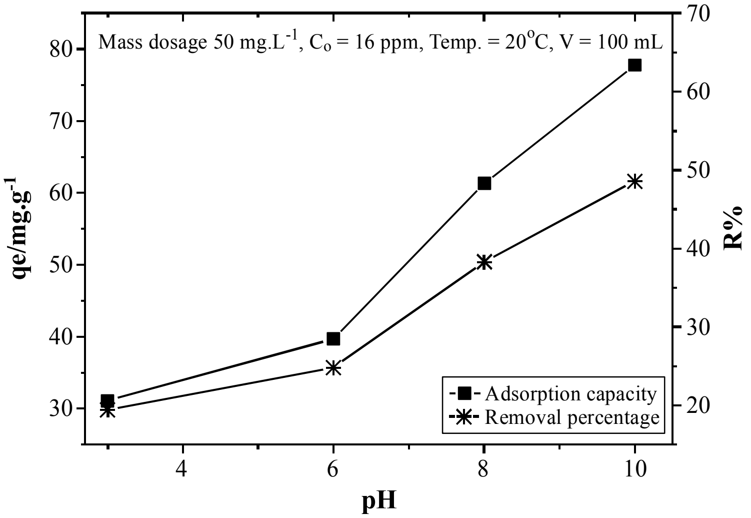

Fig. 3: Effect of initial solution pH on adsorption of BY-28 dye by ASAC surface

It was observed that the adsorption effeciency increases from 31 mg.g^{-1} (19.1%) to 77.7 mg.g^{-1} (48.6%) for an increase in pH from 3.0 to 10. Several reasons may be attributed to the adsorption of BY-28 dye by the ASAC relative to pH. The surface of the ASAC contains a large number of reactive sites, at lower pH, the surface of the ASAC gets positively charged thus making the H$^+$ ions compete effectively with dye cations causing a decrease in the amount of dye adsorbed (mg.g^{-1}). At higher pH, the surface of the ASAC gets negatively charged, which enhances the interaction of positively charged dye cations with the surface of ASAC through the electrostatic forces of attraction[26].

Effect of ASAC loading

Fig. 4 shows the plot of amount of dye adsorbed (q_e) and the (R %) dye removal against the quantity of ASAC (g) employed. From the Fig. 4, it is observed that removal efficiency (R%) increases from 25 to 33.7 % with increase in the adsorbent loading from 5 to 50 mg.L^{-1} of initial dyer concentration (16 ppm), whereas the adsorption capacity decreased from 78 mg.g^{-1} to 10 mg.g^{-1} with increase in the adsorbent loading from 5 to 50 mg.L^{-1} too. This can be attributed to an increase in surface area of the ASAC, which in turn increases the binding sites[26]. Also at higher adsorbent dosage, there is a very fast adsorption on to the adsorbent surface that leads to improved uptake of the dye[27].

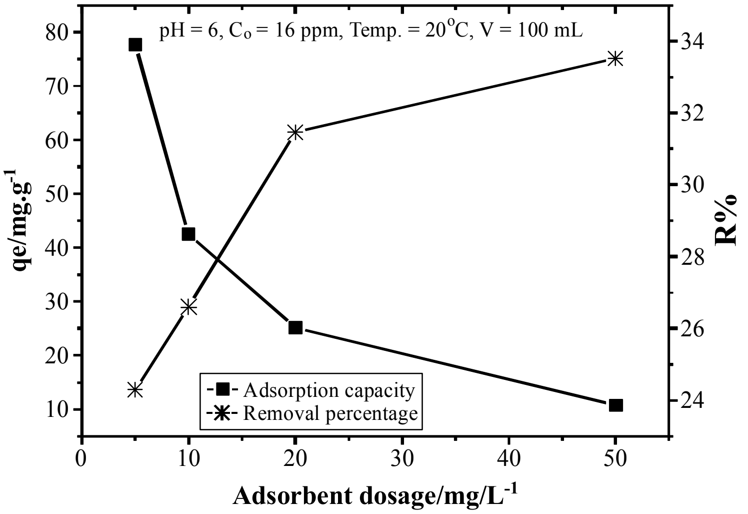

Fig. 4: Effect of initial adsorbent dosage on adsorption of BY-28 dye by using ASAC surface

Effect of initial dye concentration

Figure 5 shows the plot the quantities of dye adsorbed (*qe*) and (R%) dye removal versus initial concentration C_0 at different experimental conditions. From the Figure, it can be seen that the amount of dye adsorbed varies with varying initial dye concentration and increases with increase in initial dye concentration, but also the percentage of removal decreased with increasing in the dye concentrations[25]. An increasing the initial dye concentration increases the number of collisions between dye ions and the ASAC, which enhances the adsorption process. The effect of initial dye concentration on the ASAC capacity has been found to be of considerable significance for the basic dye used[26].

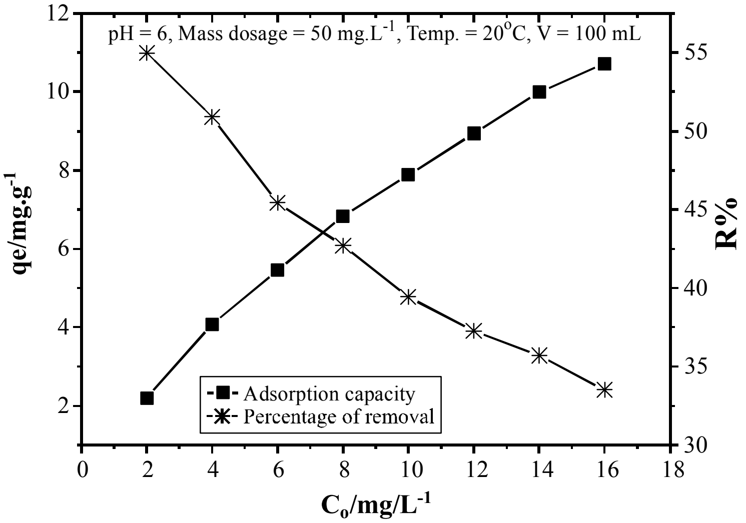

Fig. 5: Effect of initial concentration on adsorption of BY-28 dye by using ASAC surface

Effect of temperature

The adsorption experiments were carried out at (10, 20, 30 and 40°C) in order to investigate the effects of temperature on the adsorption of BY-28 onto ASAC. An acceptable increasing was obtained in the adsorption amount with increasing temperature. The adsorption efficiency increased from 27.8 mg·g^{-1} (17.38% removal) to 72.12 mg·g^{-1} (45.07% removal) for initial concentration 16 ppm of BY-28, when the temperature was increased from (10 to 40°C), results are shown in Figure 6, which indicates that the adsorption process of dye cations was endothermic in nature. It is well-known that the diffusion rate of the adsorbate molecules across the external boundary layer and in the internal pores of adsorbent particles increases and viscosity of the aqueous solution decreases by increasing the temperature of the adsorption medium[28,29].

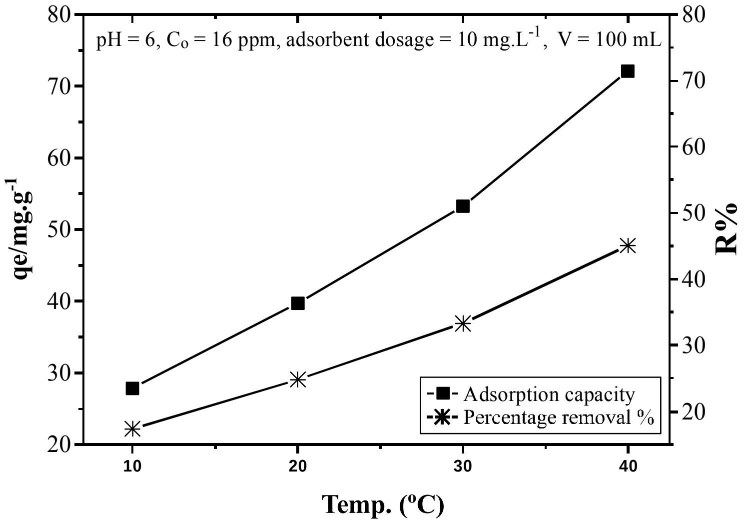

Fig. 6: Effect of solution temperature on adsorption of BY-28 dye by using ASAC surface

Thermodynamic study

The thermodynamic parameters, including the free energy changes (ΔG^0), standard enthalpy changes (ΔH^0) and the entropy changes (ΔS^0) associated with the adsorption process, can be used to deduce the adsorption mechanism. They can be calculated by the dependence of thermodynamic equilibrium constant (K_s) on temperatures[30]:

$$\Delta G_o = -RT \text{ in } K_s \qquad \ldots(3)$$

$$K_s = \frac{-\Delta H^o}{RT} + \frac{\Delta S^o}{R} \qquad \ldots(4)$$

The thermodynamic equilibrium constant (K_s) for the adsorption of BY-28 on ASAC can be calculated using the equation[31]:

$$K_s = \frac{q_e}{C_e} + \frac{v_1}{v_2} \qquad \ldots(5)$$

where v_1 is the activity coefficient of the adsorbed solute, and v_2 is the activity coefficient of the solute in equilibrium suspension. The ratio of activity coefficients was assumed to be uniform in the dilute range of the solutions[31].

As the concentration of the dye in the solution approached zero, the activity coefficient approached unity and Equation (5) became -

$$\lim_{Ce \to 0} \frac{Q_e}{C_e} = K_s \qquad \ldots(6)$$

The values of K_s determined from Figure 7, by plotting ln qe/Ce versus Ce and extrapolating to Ce = 0[31]. The calculated values of K_s and the correlation coefficients are listed in Table 2.

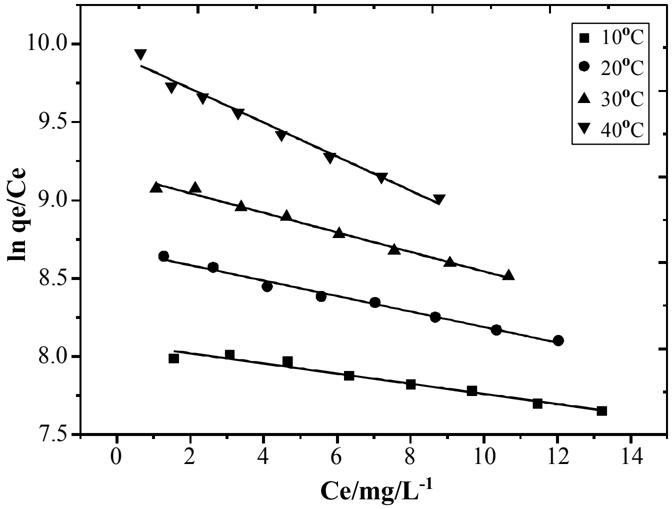

Fig. 7: Linear plots for determination of equilibrium constant (K_S) values at different temperatures

According to Equation. (3), the values of ΔG^0 were calculated and listed in Table 2. The values of ΔG^0 of dye ASAC adsorption systems are all negative, which indicates the spontaneous adsorption processes. Moreover, the increase in the absolute value of ΔG^0 with increasing temperature indicates that higher temperatures facilitated the adsorption.

The value of ΔH^0 and ΔS^0 can be calculated from the slope and intercept of the Van't Hoff plot (Equation. (4)) of ln Ks against $1/T$, respectively, and the results are listed in Table 2. The positive value of ΔH^0 indicates that the adsorptions processe are endothermic. When attraction between adsorbates and an adsorbent took place, the change in standard enthalpy was caused by various forces, including Van der Waals, hydrophobicity, hydrogen bonds, ligand exchange, dipole–dipole interactions and chemical bonds.

Table 2: Thermodynamics parameters for adsorption of BY-28 dye by ASAC surface

Temp./ ^{0}C	K_D	SE	R^2
10	8.08512	0.02105	0.95765
20	8.68406	0.01581	0.98697
30	9.17042	0.01624	0.98864
40	9.93124	0.02865	0.98102
Temp/ K	**ΔG^0/ kJ.mol^{-1}**	**ΔH^0/ kJ.mol^{-1}**	**ΔS^0/ J.K.$^{-1}$mol^{-1}**
283.15	-4.9175	4.9302	34.8024
293.15	-5.2653		
303.15	-5.5823		
313.15	-5.9740		

Models of adsorption isotherm

To investigate the parametrs dependency of the adsorption capacity, four equilibrium models were analyzed, including Langmuir, Freundlich, Redlich–Peterson and Langmuir–Freundlich. All the isotherms were simulated using an iterative procedure based on a non-linear least-squares algorithm. The Langmuir adsorption isotherm equation, expressed as follows requires for its applicability a mono-layered coverage on the surface of adsorbent[32]:

$$q_e = \frac{q_{max}\, K_L C_e}{1 + K_L C_e} \qquad \ldots(7)$$

where q_e, K_L, q_{max} and C_e are uptake at equilibrium (mg g^{-1}), the Langmuir constant (L mg^{-1}), the monolayer adsorption capacity (mg g^{-1}) and the solution concentration at equilibrium (mg L^{-1}), respectively.

The Freundlich equation is applicable for multi component adsorption. The Freundlich isotherm is expressed by[33]:

$$q_e = K_F . C_e^{\frac{1}{n}} \qquad \ldots(8)$$

where K_F is the Freundlich constant ($mg^{1-1/n} L^{1/n} g^{-1}$) and n is the Freundlich exponent.

The Freundlich equation was successfully used to fit the experimental data for many fluid–solid systems, but one of the main drawbacks of this equation is that it doesn't tend to a limiting value while the equilibrium concentration increases. The Langmuir–Freundlich equation is a way to overcome this problem[34]. It is expressed as follows:

$$q_e = \frac{q_{max}\ K_{LF} C_e^m}{1 + K_{LF} C_e} \qquad \ldots(9)$$

The Redlich–Peterson isotherm, proposed by considering the limitations of Freundlich and Langmuir isotherms[35], is given by:

$$q_e = \frac{K_{RP} C_e}{1 + a_{RP} C_e^b} \qquad \ldots(10)$$

where K_{RP} ($L\ g^{-1}$) and a_R ($L\ mg^{-1}$) are the Redlich–Peterson isotherm constants and b is the exponent.

The experimental data of BY-28 adsorption on ASAC at different conditions were well fitted by the Langmuir–Freundlich and Redlich–Peterson models.

In terms of R^2, both models provided better fitting ($R^2 > 0.994$). Figs. 8-10 present the fittings by all models equation in this study at different experimental conditions, all parameters constants are given in Table (3-6).

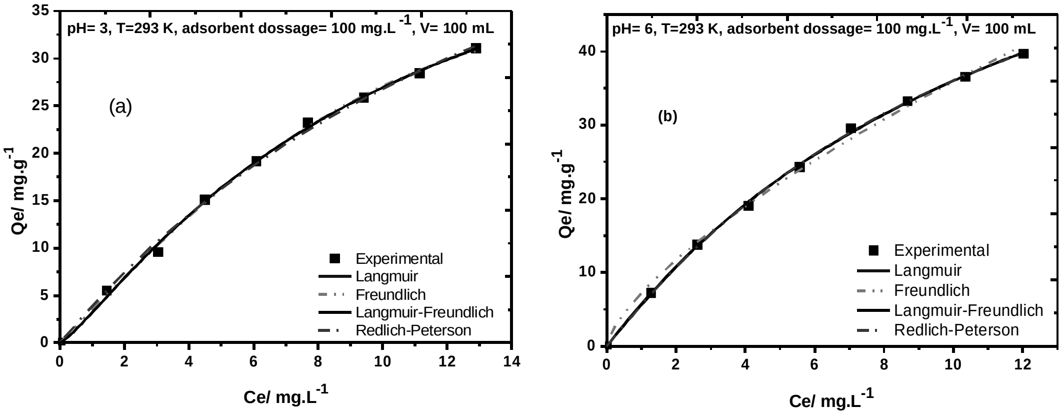

Cont…

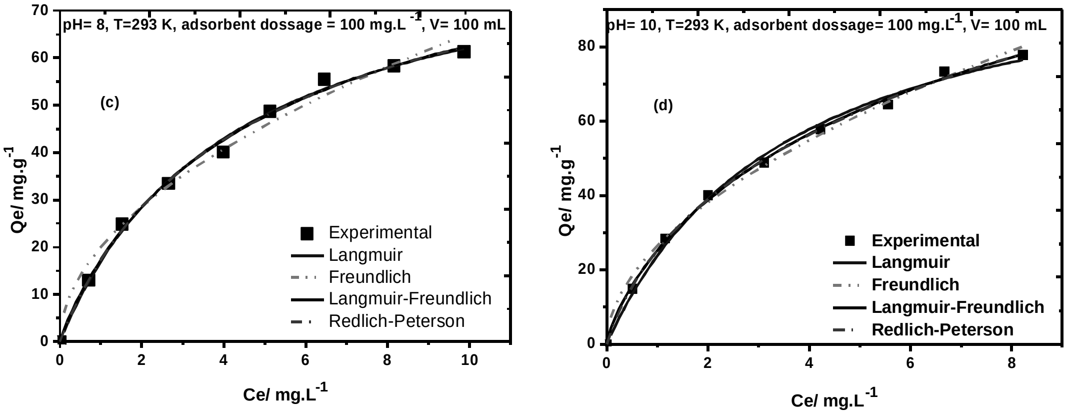

Fig. 8: Fits of the isotherm models for BY-28 on ASAC at different initial pH: a) pH3, b) pH 6, c) pH 8, and d) pH 10

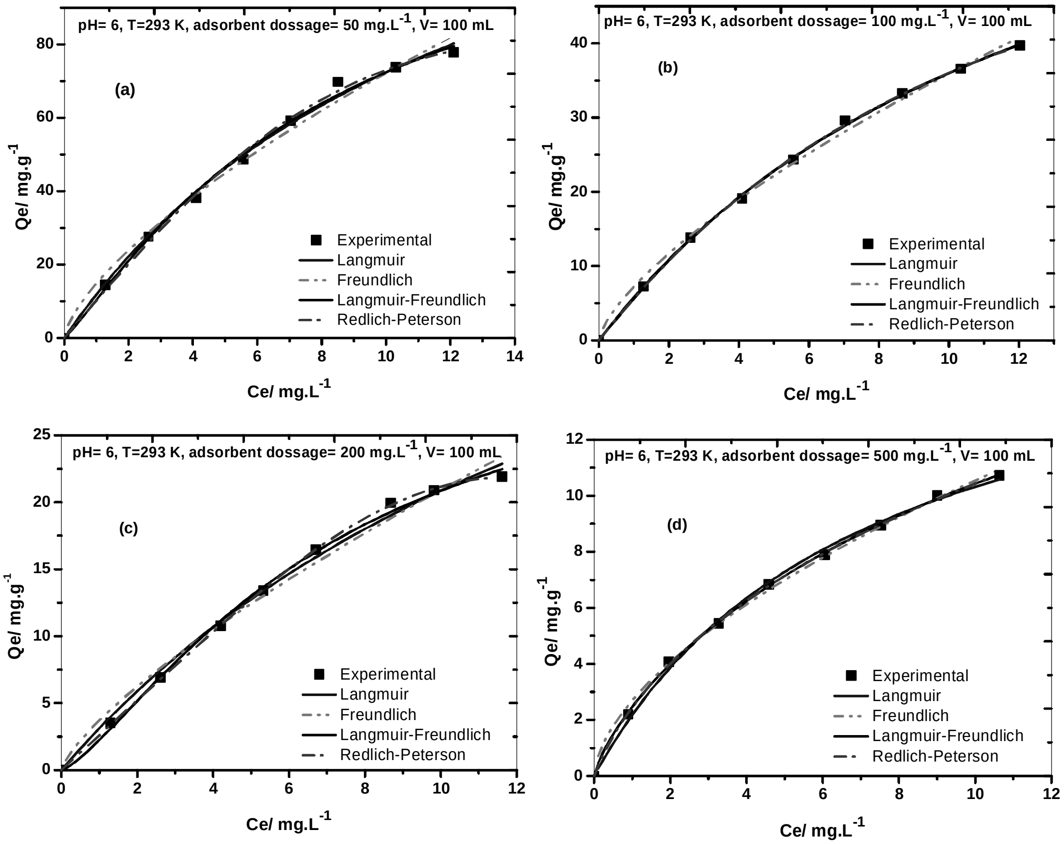

Fig. 9: Fits of the isotherm models for BY-28 on ASAC at different adsorbent dosage: a) 50 mg.L^{-1}, b) 100 mg.L^{-1}, c) 200 mg.L^{-1}, and d) 500 mg.L^{-1}

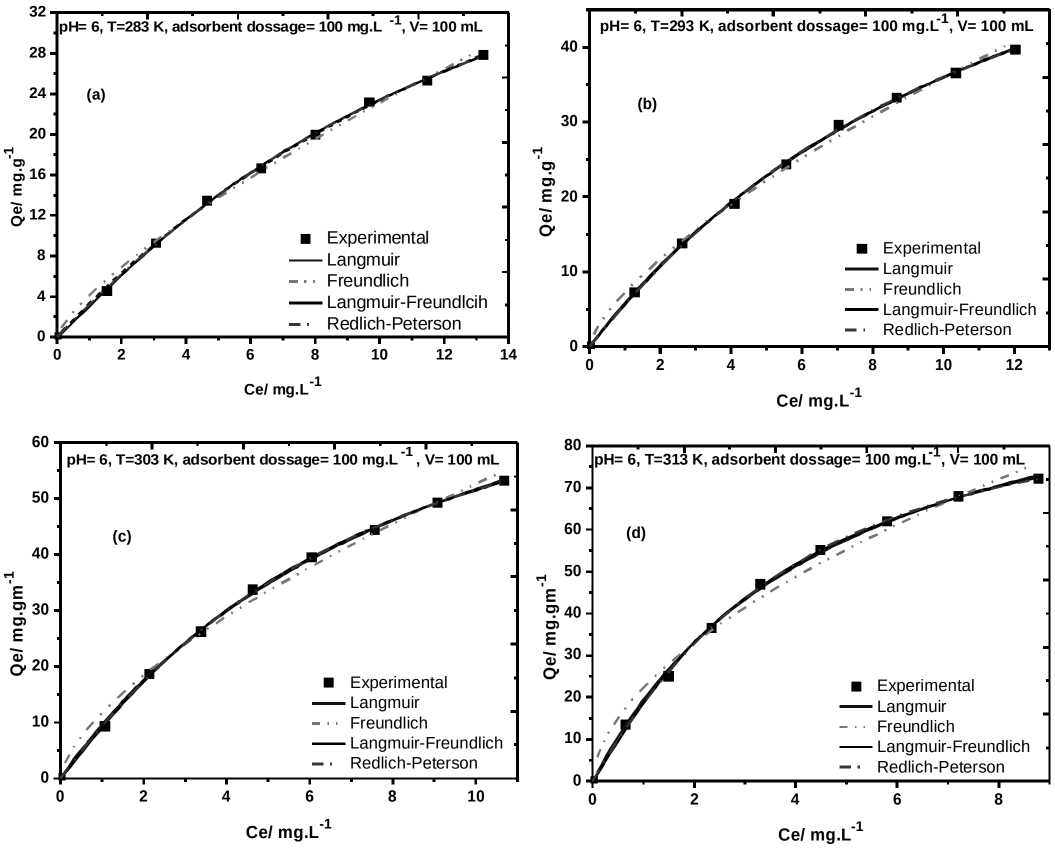

Fig. 10: Fits of the isotherm models for BY-28 on ASAC at different temperature: a) 10^0C, b) 20^0C, c) 30^0C, and d) 40^0C

Table 3: The names and non-linear forms of study isotherm model of Langmuir.

$Q_{mono} = q_{max}/K_L$

Parameters			Langmuir model constants					
pH	Temp. /K	Wt./g	q_{max} / ($mg.g^{-1}$)	SE	K_L/ ($L.mg^{-1}$)	SE	Q_{mono}/ ($mg.gm^{-1}$)	R^2
6	313	0.01	113.29	3.066	0.2064	0.011	548.8857	0.99799
	303		100.70434	2.8896	0.1055	0.00527	954.5435	0.99891
	293		85.63896	3.16096	0.07248	0.00428	1181.553	0.99883
	283		70.59856	3.40733	0.04936	0.00349	1430.279	0.99881

Cont…

Parameters			Langmuir model constants					
pH	Temp. /K	Wt./g	q_{max} / (mg.g^{-1})	SE	K_L/ (L.mg^{-1})	SE	Q_{mono}/ (mg.gm^{-1})	R^2
3	293		76.3005	6.97814	0.05407	0.00738	1411.143	0.99519
8			88.6614	4.0541	0.23491	0.02481	377.429	0.99159
10			110.38291	5.04941	0.27462	0.02872	401.9478	0.99228
6		0.02	57.11664	8.15399	0.05753	0.01208	992.8149	0.98962
		0.05	17.69442	0.81857	0.13993	0.01259	126.4519	0.99546
		0.005	166.69386	15.7684	0.07661	0.01179	2175.876	0.99156

Table 4: The names and non-linear forms of study isotherm model of Freundlich

Parameters			Freundlich model constants				
pH	Temp. /K	Wt./g m	K_F/ (mg$^{1-1/n}$. L$^{1/n}$.g^{-1})	SE	n	SE	R^2
6	313	0.01	22.304	1.6830	0.5639	0.0424	0.97576
	303		11.70357	0.8523	0.65317	0.03608	0.98716
	293		7.23477	0.4760	0.69608	0.03053	0.992
	283		4.11002	0.2895	0.74951	0.03106	0.993
3	293		4.83932	0.4601	0.73923	0.04248	0.98657
8			19.9356	1.4515	0.5145	0.03884	0.97542
10			26.46664	1.1413	0.52552	0.02522	0.99021
6		0.02	3.7031	0.4505	0.75197	0.057	0.97733
		0.05	2.69182	0.0971	0.59303	0.01805	0.99603
		0.005	14.85431	1.5550	0.68669	0.04867	0.97929

Table 5: The names and non-linear forms of study isotherm model of Langmuir-Freundlich

Parameters			Langmuir-Freundlich model constants						
pH	**Temp./ K**	**wt./g m**	**K_{LF} /(L.gm^{-1})**	**SE**	**a_{LF} /(L.mg^{-1})**	**SE**	**n_{LF}**	**SE**	**R^2**
6	313	0.01	22.69353	0.6966	0.22174	0.0113	1.1019	0.0556	0.99911
	303		10.063	0.3219	0.11406	0.0048	1.0899	0.0420	0.99957
	293		6.05979	0.3065	0.07527	0.0062	1.0311	0.0578	0.99921
	283		3.20481	0.1733	0.05565	0.0037	1.0902	0.0519	0.99943
3	293		3.44296	0.3921	0.0634	0.0054	1.1908	0.1057	0.99776
8			21.2544	1.3747	0.2192	0.0373	0.9196	0.1216	0.99489
10			29.98862	1.2233	0.19047	0.0433	0.7780	0.0781	0.99769
6		0.02	2.39236	0.3543	0.06975	0.0066	1.3475	0.1389	0.99645
		0.05	2.69028	0.0642	0.0929	0.0166	0.7823	0.0471	0.99932
		0.005	11.26067	1.5965	0.08493	0.0106	1.1510	0.1484	0.99499

Table 6: The names and non-linear forms of study isotherm model of Redlich–Peterson

Parameters			Redlich–Peterson model constants						
pH	**Temp./ K**	**Wt./g m**	**k_{RP}/ (L.gm^{-1})**	**SE**	**a_{RP}/ (L.mg^{-1})**	**SE**	**b**	**SE**	**R^2**
6	313	0.01	20.52368	0.8887	0.11004	0.0253	1.2018	0.0772	0.99938
	303		9.8736	0.4654	0.06414	0.0219	1.1546	0.1089	0.99946
	293		5.86802	0.3420	0.04544	0.0236	1.1411	0.1604	0.99927
	283		3.25051	0.1627	0.02178	0.01473	1.2503	0.2128	0.99934
3	293		3.53986	0.1877	0.00531	0.0064	1.7619	0.4210	0.99805
8			22.75202	4.4713	0.31496	0.18431	0.9225	0.1466	0.99472
10			46.39096	9.8911	0.83087	0.3523	0.7312	0.0793	0.99803
6		0.02	2.60548	0.0244	9.678E-5	5.922E-5	3.3777	0.2394	0.99974
		0.05	6.45883	1.2661	0.6086	0.2158	0.6577	0.0622	0.9994
		0.005	10.26022	0.6128	0.0047	0.0059	1.9356	0.4582	0.99657

CONCLUSION

The adsorption equilibrium of the BY-28 dye on the ASAC was studied in a batch mode operation for the parameters initial dye concentration, pH, temperature, and adsorbent dosage. The results showed that adsorption of the dye increased with increase in initial dye concentrations,temperature and pH while it decreased with increase in adsorbent mass. The adsorption equilibrium isotherms were analyzed by Langmuir, Freundlich, Langmuir-Freundlich and Redlich–Peterson isotherm equations. All results obeying isotherm models were choosing in this study but more favourable for Langmuir-Freundlich and Redlich–Peterson isotherms, which provided the best correlations for the BY-28 dye onto ASAC.

As a result of the thermodynamic evaluation of BY-28 adsorption, the obtained negative ΔG values revealed that the adsorption of BY-28 onto ASAC was thermodynamically feasible and spontaneous, the positive values of ΔH suggested the endothermic nature of adsorption, and the positive values of ΔS indicated the increasing randomness at the solid/solution interface during the adsorption process.

ACKNOWLEDGEMENT

The authors are highly thankful to Chemistry Department, Faculty of Girls Science, Babylon University for providing laboratory facilities and for support of this work.

REFERENCES

1. E. C. T. Forgacs and G. Oros, Environ. Int., **30**, 953-971 (2004).
2. X. H. Wu, K. N. K. S. Hui, S. K. Lee, W. Zhou, R. Chen, D. H. Hwang, Y. R. Cho and Y. G. Son, Chem. Eng. J., **180**, 91-98 (2012).
3. T. D. Nguyen, C. T. Dinh and T. O. Do, Nanoscale, **3**, 1861-1873 (2011).
4. M. Kobya, E. Demirbas and E. Senturk, M. Ince, Bioresour. Technol., **96**, 1518-1521 (2005).
5. M. Ceron-Rivera, M. M. Davila-Jimenez and M. P. Elizalde-Gonzalez, Chemosphere, **55**, 1-10 (2004).
6. J. Guo and M. Wang, Plant Growth Regul., **62**, 1-8 (2010).
7. S. Yang, S. Chen, Y. Chang, A. Cao, Y. Liu and H. Wang, J. Colloid Interface Sci., **359**, 24-29 (2011).
8. K. S. Hui and C. Y. Chao, J. Hazard. Mater., **137**, 401-409 (2006).

9. K. S. Hui, C. Y. Chao and S. C. Kot, J. Hazard. Mater., **127**, 89-101 (2005).

10. S. Noonpui, P. Thiravetyan, W. Nakbanpote and S. Netpradit, Chem. Eng. J., **162**, 503-508 (2010).

11. D. Rameshraja, V. C. Srivastava, J. P. Kushwaha and I. D. Mall, Chem. Eng. J., **181-182**, 343-351 (2012).

12. V. K. Gupta, I. Ali, D. Suhas and J. Mohan, Colloid Interface Sci., **265**, 257-264 (2003).

13. A. Mittal, D. Jhare and J. Mittal, J. Mol. Liq., **179**, 133-140 (2013).

14. M. Ozacar, İ. A. Sengil, Bioresour. Technol., **96**, 791-795 (2005).

15. P. K. Malik, Dyes and Pigments, **56**, 239-249 (2003).

16. S. T. Ong, C. K. Lee and Z. Zainal, Bioresour. Technol., **98**, 2792-2799 (2007).

17. Y. Ho, W. Chiu, C. Wang, Bioresour. Technol., **96**, 1285-1291 (2005).

18. E. Demirbas, M. Kobya, S. Oncel and S. Sencan, Bioresour. Technol., **84**, 291-293 (2002).

19. D. Kavitha and C. Namasivayam, Bioresour. Technol., **98**, 14-21 (2007).

20. A. Jumasiah, T. G. Chuah, J. Gimbon, T. S. Y. Choong and I. Azni, Desalination, **186**, 57-64 (2005).

21. T. Robinson, B. Chandran and P. Nigam, Environment International, **28**, 29-33 (2002).

22. E. Demirbas, M. Kobya and M. T. Sulak, Bioresour. Technol., **99**, 5368-5373 (2008).

23. M. Soleimani and T. Kaghazchi, Bioresour. Technol., **99**, 5374-5383 (2008).

24. A. C. Ueda, L. H. de Oliveira, N. Hioka and M. Aznar, J. Chem. Eng. Data, **56**, 652-657 (2011).

25. T. K. Abd El Hakim, A. S. Ebtssam, A. A. Ayman and E. A. Amir, European J. Chem., **1**, 99-105 (2012).

26. R. Aravindhan, J. R. Rao and B. U. Nair, J. Hazard. Mater., **142**, 68-76 (2007).

27. S. Jodeh, European J. Chem., **4**, 468-474 (2012).

28. M. Alkan, M. Dogan, Y. Turhan, O. Demirbas and P. Turan, Chem. Eng. J., **139**, 213-223 (2008).

29. C. Duran, D. Ozdes, A. Gundogdu and H. Senturk, J. Chem. Eng. Data, **56**, 2136-2147 (2011).

30. Q. Li, Q. Yue, Y. Su, B. Gao and H. Sun, Chem. Eng. J., **158**, 489-497 (2010).
31. V. K. Gupta, P. Singh and N. Rahman, J. Colloid Interface Sci., **275**, 398-402 (2004).
32. I. Langmuir, J. Am. Chem. Soc., **40**, 1361-1403 (1918).
33. H. M. Freundlich, Zeitschrift für Physikalische Chemie, **57A**, 385-470 (1906).
34. R. Sips, J. Chem. Phys., **16**, 490-495 (1948).
35. O. Redlich and D. L. Peterson, J. Phys. Chem., **63**, 1024-1024 (1959).

Accepted : 22.03.2013